Environ Earth Sci (2014) 71:1699–1710
DOI 10.1007/s12665-013-2574-x

ORIGINAL ARTICLE

The water transfer properties and drying shrinkage of aerial lime-based mortars: an assessment of their quality as repair rendering materials

Arizzi Anna · Cultrone Giuseppe

Received: 10 January 2013 / Accepted: 20 May 2013 / Published online: 5 June 2013

Abstract Water (in the solid, liquid and vapour state) is one of the main factors that drive construction materials to deterioration. To assess the quality and durability of a repair rendering mortar, thus ensuring its protective function in the masonry structure, it is fundamental to study the behaviour of this mortar towards water. Mortars were elaborated with a calcitic dry hydrated lime, a calcareous aggregate, a pozzolan, a lightweight aggregate, a water-retaining agent and a plasticiser. The effect of different binder-to-aggregate proportions on the mortars' hygric behaviour was assessed by performing free water absorption and drying, capillary uptake, hydraulic conductivity and water vapour permeability tests. Another aspect that was considered in the assessment of mortar quality was the drying shrinkage that was measured by means of a non-standardised device. It has been found that a larger amount of water is absorbed by mortars with higher lime content, whilst faster drying and higher permeability to water and water vapour are obtained in mortars with higher aggregate content. The hygric behaviour as well as the drying shrinkage of mortars has been interpreted taking into account the differences in microstructure and pore system between mortars.

Highlights: study of the quality of rendering mortars/assessment of the hygric properties of mortars according to their dosage/influence of the interfacial transition zone on the mortar permeability and shrinkage.

A. Anna (✉) · C. Giuseppe
Departamento de Mineralogía y Petrología, Universidad de Granada, Campus Fuentenueva s/n, 18002 Granada, Spain
e-mail: arizzina@ugr.es

C. Giuseppe
e-mail: cultrone@ugr.es

Keywords Lime mortars · Water uptake · Drying · Permeability · Drying shrinkage · Interfacial transition zone

Introduction

In the last decades, many investigations have been carried out to understand the mechanisms of deterioration driven by water in building materials (Rose 1963a, b; Vos 1978; Scherer 1990; Rojo et al. 2003). Processes like moisture gas diffusion (Beck et al. 2003), rising damp (Beck et al. 2003; Hall and Hoff 2007), draining rain (Groot and Gunneweg 2010), freezing–thawing phenomena (Ingham 2005), salt transport and crystallisation (Cultrone and Sebastián 2008; Ruiz-Agudo et al. 2011; Szemerey-Kiss and Torok 2011) and biodeterioration (Warscheid and Braams 2000) occur in the majority of the historic and modern buildings all over the world.

The practice of rendering, i.e. covering a wall or a building façade with one or more layers of mortar, has the main aim to protect the masonry structure against the processes above mentioned, which are all driven by water (Hall and Hoff 2007; Groot and Gunneweg 2010; Wood 2010). Repair mortars, in general, are considered "sacrificial" materials because, as explained by Maurenbrecher (2004), "it is easier to repair mortar joints than replace masonry units". In the same way, a rendering mortar must act as a "sacrificial layer" that fulfils a protective function towards the substrate (stone, brick, concrete). Therefore, to evaluate the quality and durability of a rendering mortar, thus ensuring its protective function in the masonry structure, it is fundamental to assess the behaviour of this mortar towards water.

In the case of structural (with a "joining" function) or rendering mortars, the water absorption should be not very

different to that of the existing masonry materials (Maurenbrecher 2004; Hughes 2010), so as to ensure a homogeneous flow of water through different materials, to avoid the localisation of water in certain zones of the masonry (which would lead it to a faster deterioration). In addition, water vapour transmission rates should be higher to enable drying through the mortar (Groot 2010). In practice, the drying of a porous surface occurs in two stages: the early stage, which depends mainly on the conditions of temperature, relative humidity and ventilation, and the later stage that is determined primarily by the water transfer properties of the material (Hall and Hoff 2002), which in turn depend on its pore system (i.e. pore size and interconnection among pores) (Scherer 1990). This explains the importance of ensuring a fast drying kinetics in a rendering mortar.

The aim of this work was to assess the water transfer properties of aerial lime-based mortars designed for rendering purposes. Four types of mortars were elaborated with a pozzolanic additive (metakaolin), a lightweight aggregate and two admixtures. The addition of a pozzolan to lime-based mortars is advisable to guarantee better durability and physical–mechanical properties (Veiga 2010). Metakaolin, in particular, is one of the most used pozzolans because of its high degree of reactivity (Frías et al. 2000). The lightweight aggregate and the two admixtures, a water-retaining agent and a plasticiser, were used to improve the behaviour of mortars in the fresh state. Mortars have been elaborated with different binder-to-aggregate ratios to determine which dosage gives place to a mortar with the best hygric behaviour. Indeed, it is known that depending on the binder-to-aggregate proportion, different texture, porosity, compactness and mechanical strengths are obtained in lime-based mortars of similar composition (Lanas and Alvarez 2003; Arizzi and Cultrone 2012; Arizzi et al. 2011, 2013); therefore, it is expected that also the behaviour towards water changes according to the aggregate proportions, as well as the mortar durability (Arizzi et al. 2012). For this purpose, we studied the relationship between hygric behaviour and mortar microstructural characteristics. Indeed, the water transfer through a mortar is influenced by its pore system; in particular, main pore size and shape are the factors that mostly determine the amount of water absorbed and the kinetics of absorption/desorption (Scherer 1990; De La Torre 2003). Moreover, by performing different hygric tests, we also aim to investigate more in deep why a mortar with low content of aggregate turns to be more resistant to the superficial attack of a salt solution, whilst a mortar with high lime proportion shows a stronger decay to water/salt solution absorption by capillarity (Arizzi et al. 2012).

Finally, there is another factor that is not taken into account during the hygric tests but which plays an important role in the water transfer properties of a rendering mortar: the shrinkage. This process, caused by the rapid evaporation of the kneading water (i.e. water added to the mortar mixture) with the final formation of cracks, is especially strong in aerial lime-based mortars, which need more water for their mixing. On the one hand, shrinkage is a negative aspect for mortar durability since it gives place to open ways of access through which water can enter and diffuse easily. On the other hand, the presence of shrinkage fissures allows maintaining water moisture diffusion from the substrate to the surface (Benavente et al. 2009). These factors are rarely taken into consideration during the hygric tests performed in laboratory, since mortar samples of $4 \times 4 \times 16$ or $4 \times 4 \times 4$ cm in size do not undergo such degree of shrinkage. For this reason, the mortar shrinkage in large samples was also studied here and then considered in the final assessment of mortar hygric properties.

Materials and methods

Mortars preparation

Four mortar types were elaborated with the following components: a calcitic dry hydrated lime (CL90-S (UNE EN 459-1 2002); ANCASA, Seville, Spain), a calcareous aggregate (CA $0.063 < \varnothing < 1.5$ mm), a metakaolin (CLASS N POZZOLAN (ASTM 2008); Burgess Pigment Company, USA), a lightweight aggregate (perlite) and two different admixtures, a water-retaining agent (cellulose derivative) and a plasticiser (polycarboxylate) (additional detail of these components can be found at http://www.argosdc.com). The mortars have been labelled CCMPCR3, CCMPCR4, CCMPCR6, CCMPCR9, according to their binder-to-aggregate (B/A) ratio (1:3, 1:4, 1:6 and 1:9 by weight, respectively); the pozzolan was kept at 10 % of the total binder (by weight) and the total amount of lightweight aggregate and admixtures was less than 2 % of the total weight, since these proportions were found to be the most suitable for rendering mortars (Arizzi and Cultrone 2012). The fresh mortar pastes had a flow comprised between 120 and 150 mm (UNE EN 1015-3 1999). The components and dosages used in each mortar are shown in Table 1. Mortars were conserved during 7 days in normalised steel moulds ($4 \times 4 \times 16$ cm) at $T = 20 \pm 5$ °C and RH $= 60 \pm 5$ %, instead of being cured at a RH of 95 %, following the modification of the standard UNE EN 1015-11 (1999) proposed by Cazalla (2002). After demoulding, they were cured at the same conditions of T and RH for 60 days in total. The petrographic characteristics and mechanical properties of these mortars have been published elsewhere (Arizzi and Cultrone 2012).

Table 1 Proportions of components used in the elaboration of the four mortar types

Mortars name	Components name and proportions			Water
	B/A	MK	P + C + R	
CCMPCR3	1:3	10	<2	28.0
CCMPCR4	1:4	10	<2	26.5
CCMPCR6	1:6	10	<2	21.5
CCMPCR9	1:9	10	<2	20.0

The total amount of admixtures (P + C + R) is in % of the total weight of mortar. The amount of kneading water (as % of the total weight) was determined to obtain a paste with a flow comprised between 120 and 150 mm

B/A binder-to-aggregate ratio (by weight), *MK* metakaolin (in % of the total weight of the binder), *P* perlite, *C* cellulose derivative, *R* polycarboxylate

Hygric tests

Free water absorption, drying, capillary imbibition, hydraulic conductivity and water vapour permeability tests were performed to study the hygric properties of mortars. Hygric tests were not performed until the mortars had been cured for 60 days, because "younger" mortars are less compact and lime dissolves in water. Mortar samples were oven-dried at 90 °C for 24 h to ensure a total drying of the samples, as needed for the hygric tests.

Free water absorption and drying

The absorption and drying kinetics were determined on three samples (4 × 4 × 4 cm) per type by measuring the changes in the weight of mortar samples over time, due to the movements of water within the pore system. The absorption coefficient (C_a) was determined as the slope of the curve representing the weight increase as a function of the square root of time 4 min after the beginning of the test (UNI-EN 13755 2008). The drying index (I_d) was measured according to the NORMAL 29–88 (1988).

Capillary uptake

Capillary rise was performed on three samples of 4 × 4 × 16 cm, according to the UNI EN 1925 (2000). Two imbibition coefficients (C_u and C_f) were determined from the weight uptake per surface unit and the height over time, following the Beck et al. (2003) procedure.

Hydraulic conductivity

The hydraulic conductivity (or permeability to water) of mortars was determined with the falling head method, by means of the experimental apparatus performed by Domenico and Schwartz (1990).

Prior to the experiment, prismatic samples 2 × 4 × 4 cm in size were polished to reduce as much as possible the roughness of the surface and their edges were rounded off (Fig. 1a). This was necessary for the next preparation step, in which samples were wrapped in a single length PTFE tape (plumber's thread sealing tape) to create at least ten overlapping layers that completely covered the largest surface of the sample (Fig. 1b). To compress the tape layer into the surface of the mortar and produce a watertight sleeve, samples were then encapsulated with electrician's heat shrinkable sleeving (Fig. 1c). The heat shrinkable sleeving was shrunken with a hot-air gun to its minimum diameter. The water flow during the permeability test occurs only in one direction, through two parallel surfaces of the samples. Samples were stored under water for 1 day and then completely saturated under vacuum before the test. After this, each sample was connected to the standpipe of the falling head permeameter (Fig. 1d) using a rubber bung that was pushed into the sleeving of the prepared sample (Fig. 1e). The height was recorded from the water level in the trough, in which the samples were kept submerged. During this test, the water flow through the pore network of the sample is possible, thanks to the atmospheric pressure acting on the water in the standpipe.

The time required for a given change in head at different intervals was noted manually and used in Eq. (1) to determine hydraulic conductivity. This equation derives from equating flow through the tube with flow through the sample:

$$K_h = \frac{aL}{At} \ln\left(\frac{h_1}{h_2}\right) \quad (1)$$

where K_h is the hydraulic conductivity (in ms^{-1}), a is the cross-sectional area of the tube (m^2), L is the length of sample (m), A is the cross-sectional area of the sample (m^2), t is the time (s) taken for head fall from initial head h_1 to final head h_2, as shown in Fig. 2.

Water vapour permeability

The water vapour permeability (K_v, in $g\ m^{-2}\ h^{-1}$) was determined on three samples (1.5 × 4 × 4 cm) per mortar type. Afterwards, they were placed in experimental permeameters (Fig. 3a) filled with deionised water, avoiding the contact of water with the sample surface (Fig. 3b). Permeameters were then sealed using dishes of silicon rubber (Fig. 3b). The water vapour permeability assay was performed for 5 days in total, at controlled conditions ($T = 25$ °C; RH = 40 ± 5 %). The whole weight (permeameter + sample + water) was recorded over 24 h intervals and a lineal trend curve was obtained from the

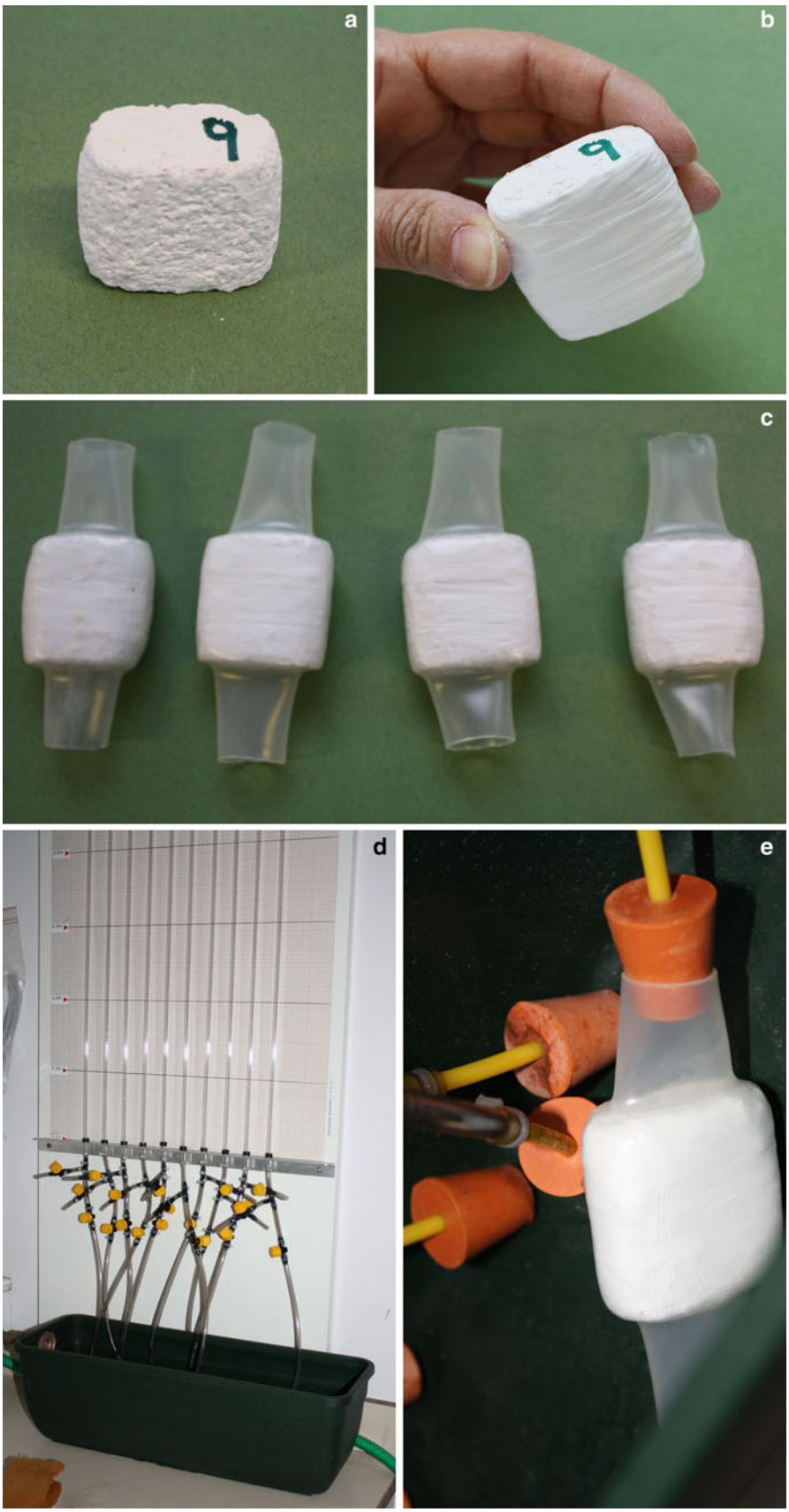

Fig. 1 Falling head water permeability test. **a** Polished and smoothed sample; **b** sample covered with PTFE tape along the largest surface; **c** aspect of the samples after being encapsulated with electrician's heat shrinkable sleeving; **d** falling head permeameter; **e** connection of the sample to the standpipe using a rubber bung

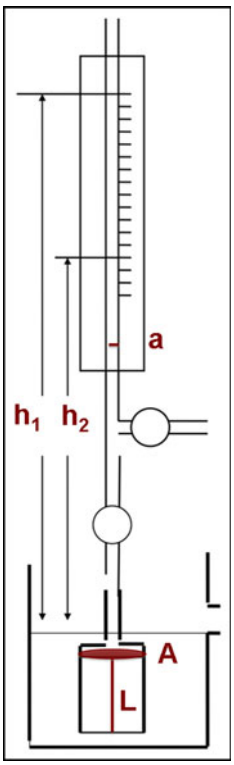

Fig. 2 Scheme of the falling head permeameter used to determine the hydraulic conductivity of mortars: *a* cross-sectional area of the tube (m^2), *L* length of the sample (m), *A* cross-sectional area of the sample (m^2), h_1 and h_2, initial and final head

weight drop over time. Following the Darcy's law, the equation applied to calculate the water vapour permeability of mortars was:

$$K_v = \frac{\frac{\Delta M}{S}}{t} \times 0.7378 \cdot L \quad (2)$$

where $\Delta M/S$ is the weight variation of the permeameter + sample + water per surface unit (surface of the sample exposed to vapour, equal to 0.000707 m^2, Fig. 3b), *t* the duration time of the test, 0.7378 a correction factor applied to determine the K_v value at $T = 20$ °C (as established in the NORMAL 21/85, 1985) and *L* is the sample thickness (Fig. 3b). The correction factor was determined by adjusting the vapour pressure at 20 °C ($P_{20} = 17.53$ mmHg).

Samples dimensional variations (shrinkage)

A SWG-H-400 shrinkage-measuring device (Fig. 4a) was used to measure the initial shrinkage of mortars. This apparatus measures the horizontal dimensional variations of a fresh mortar, by means of two sensors connected to a PC (Fig. 4b).

The internal surfaces of the apparatus (prism of 7 × 7 × 7 cm, 40 cm long, Fig. 4b) were covered with a polyethylene film to ease the mortar removal after the measurement. The fresh mortar mixture (~3 kg) was poured into the apparatus and the sensors were connected to the two extremities. These sensors recorded the length of the mortar sample every 5 min during 7 days and data were collected simultaneously by a computer. This allowed obtaining a curve of shrinkage over time, the slope of which corresponded to the shrinkage coefficient (C_{shr}, mm/h). In addition, the shrinkage percentage on the length of the sample measured was determined.

Results and discussion

Hygric behaviour of mortars

The possible alteration of mortar microstructure due to the reactions with water has been taken into account in the interpretation of the hygric behaviour of mortars.

Free water absorption and drying

The water absorption curves (Fig. 5a) show a first section with sharp slope, which indicates fast water absorption within the first few hours, and a second section with a very slight, almost plane, slope, which suggests that mortars continued absorbing water at a much lower rate during the following 15 days, until reaching a constant weight. The presence of trapped water in the mortars' pore network may have produced this slow final absorption rate (Hall and Hoff 2002). The absorption coefficient (Table 2) values indicate that mortars with higher lime content presented higher water absorption. As shown in the inset of Fig. 5a, CCMPCR3 mortar samples absorbed water slower than CCMPCR4 during the first 4 min and this is reflected in the C_a value of this mortar. This different absorption rate at the beginning of the test is due to the fact that CCMPCR3 is characterised by a larger amount of metakaolin, i.e. of reactive phases that turn into hydrated phases if they react with water; this would produce some changes in the microstructure, thus giving place to an initial water absorption slightly slower than the expected. This fact confirms the modifications of microstructure produced by the formation of hydrated phases: when further hydration occurs, the volume of smallest pores [in the range between 0.01 and 0.1 μm (Arizzi and Cultrone 2012)] increases, with a consequent decrease of mortar water absorption rate (Mamillan 1981; Benavente et al. 2002; Hall and Hoff 2002). This is, in fact, what occurred in CCMPCR3 samples. However, after the first few minutes, the water uptake is the highest in CCMPCR3 that, indeed, is characterised by the highest volume of pores (P_o, Table 2).

During the water absorption test, a small quantity of material was lost from the mortar samples, especially CCMPCR9. In general, this occurred because mortars were only partially carbonated after 2 months and the lime

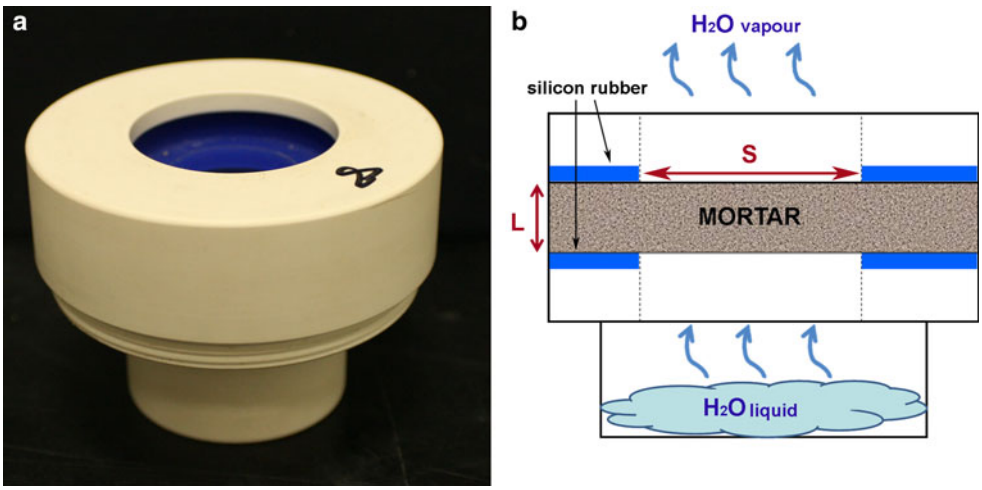

Fig. 3 Image (**a**) and scheme (**b**) of a permeameter used to determine the permeability to water vapour of mortars: *L* thickness of the sample, *S* surface of the sample exposed to the air

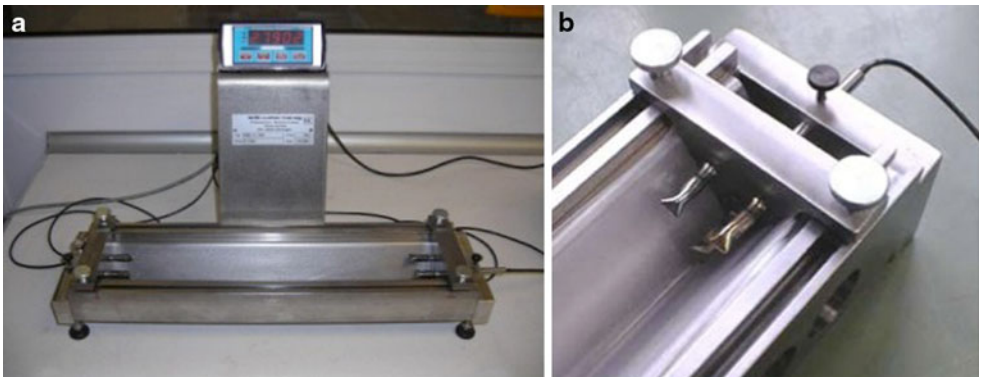

Fig. 4 SWG-H-400 shrinkage-measuring device: general image (**a**) and detail of the internal surfaces and the sensors (**b**) connected from the extremities of the apparatus to a PC

partially dissolved in water during the test. In fact, according to Arizzi and Cultrone (2012), a 10 ± 4 % of portlandite is still present in CCMPCR mortars after 2 months since their elaboration, being in larger amount in mortars with higher initial content of lime. In the specific case of CCMPCR9 mortar, we observed the loss of some aggregate grains from the sample surface, similar to the superficial decay already observed in lime mortars with high aggregate content subjected to salt deposition (Arizzi et al. 2012). This confirms the main role that water plays in worsening the cohesion between the aggregate grains and the matrix in this mortar due to the partial dissolution of portlandite.

Interestingly, the highest value of drying index was obtained in CCMPCR9 mortar, whilst the other mortars presented similar values among them (Table 2) and a very similar drying behaviour, as reflected in the slopes of their drying curves (Fig. 5b). The main difference that can be observed from the drying curves is that only in CCMPCR9 samples the final weight variation reached zero, whilst the other curves remained asymptotical over the *x*-axis. The trend of the curve and the value of I_d found for CCMPCR9 mortar indicate that water evaporates slightly faster in this mortar than in the others. However, this result is just an artefact as a consequence of the material loss suffered by CCMPCR9 samples during the water absorption test, which was due to a poorer binding ability of the matrix with consequent modifications of the real drying behaviour of the mortar.

Capillary uptake

The four mortars showed the same behaviour towards the capillary uptake as towards the water absorption, being the mortars with the highest lime content those which absorbed the highest amount of water by capillarity. This behaviour towards water coincides with the worse resistance to salt capillary uptake of mortars with high lime content (Arizzi et al. 2012). Moreover, a similar trend between the water absorption and capillary uptake curves can be recognised in CCMPCR3 and CCMPCR4 mortars (Fig. 5a, c). During the first 5 h (Sect. 1 in the capillary curves, Fig. 5c), these two mortars showed the same capillary uptake (see C_u values in Table 2); then, within the following day (curve

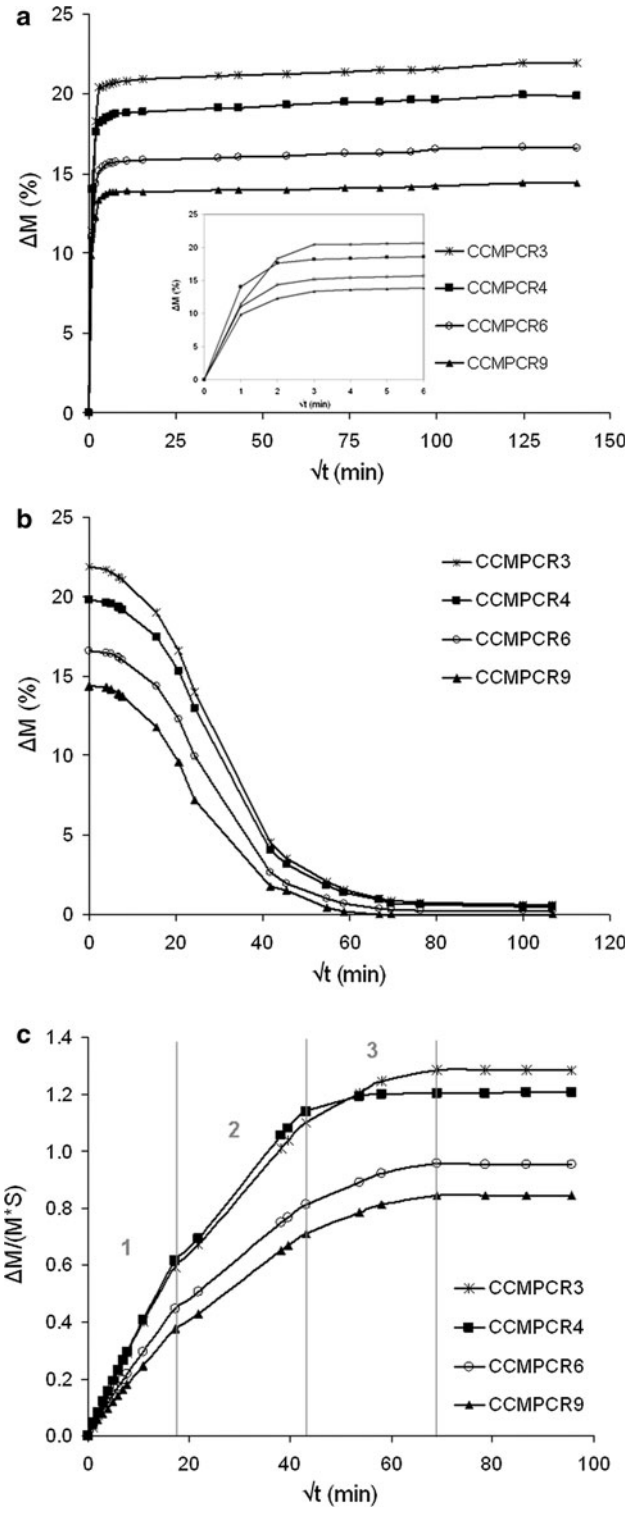

Fig. 5 Free water absorption (**a**), drying (**b**) and capillary uptake (**c**) curves of mortars after 60 days of carbonation. In the water absorption and drying curves, the weight variation (ΔM, g) is represented as function of the square of time ($\sqrt{t}$, $min^{-1/2}$). The *inset* in **a** shows the first section of the water absorption curves. In the capillary uptake curve, the weight increase (ΔM, g) per surface unit (S, m^2) (**c**) is represented as function of the square of time ($\sqrt{t}$, $min^{-1/2}$)

Table 2 Open porosity (P_o, in %) of the external (Ex) and internal (In) zones of samples; absorption coefficient (C_a, $g/min^{1/2}$), drying index (I_d) and imbibition coefficients (capillary uptake, C_u, g/cm^2 $min^{1/2}$ and capillary front, C_f, $cm/min^{1/2}$) of the four mortar samples

Mortar name	MIP analysis[a]		Hygric tests			
	Zone	P_o	C_a	I_d	C_u	C_f
CCMPCR3	Ex	37.8 ± 4.1	9.61	0.486	0.036	6.80
	In	39.9 ± 6.2				
CCMPCR4	Ex	33.1 ± 0.1	9.84	0.489	0.042	7.47
	In	35.9 ± 0.3				
CCMPCR6	Ex	30.9 ± 0.1	7.95	0.458	0.033	5.13
	In	32.7 ± 0.2				
CCMPCR9	Ex	30.4 ± 1.3	6.89	0.526	0.030	–
	In	32.2 ± 0.5				

C_f value was not calculated for CCMPCR9 mortar

[a] Values according to Arizzi and Cultrone (2012)

Sect. 2, Fig. 5c), CCMPCR4 absorbed water faster than CCMPCR3, although at the end of the test (curve Sect. 3, Fig. 5c) the latter absorbed more water. As mentioned in "Free water absorption and drying", the little difference observed in the capillary kinetics of these two mortars is the result of the formation of more hydrated phases in CCMPCR3 mortar due to the contact of reactive phase with water during the test. However, it is difficult to prove the increase of hydrated phases by means of mineralogical analysis carried out on the same samples after the hygric tests, since these phases (CSH, CAĈH and CAH) are mostly amorphous or semi-crystalline with low-reflecting power.

A considerably lower (Fig. 5c) and slower capillary uptake (C_u values in Table 2) occurred in CCMPCR6 and CCMPCR9 mortars, because of their lower porosity (Table 2).

Determining the position of the capillary front in mortars was a difficult task because the white colour of the mortar samples did not enable a precise lecture, especially in CCMPCR9, where the presence of more aggregate grains made this determination harder; in this mortar, in fact, the C_f value was not determined (Table 2). Mixing the water with a dye would have facilitated the evaluation of the capillary front in mortars, but it might have introduced ions that could interact with the chemical compounds of mortars (lime, metakaolin, admixtures) as well as it would have changed the density of the fluid, thus influencing the interpretation of the water transfer through the samples. To avoid further modifications of the mortar, which in itself is a material that constantly changes over time, and to maintain the same methodology for all samples, we have preferred not to use any dye for this test.

The C_f value can be linked to the value of sorptivity, a parameter that is widely considered to characterise the microstructure and durability of cement-based mortars (Hall and Hoff 2002). The lime-based mortars studied here present a value of sorptivity that approaches quite well that of other building materials, such as limestones, sandstones and plasters (De La Torre 2003).

Hydraulic conductivity

The range of hydraulic conductivity values obtained for the four mortars is between 10^{-6} and 10^{-5} m/s, which is between 3 and 6 orders of magnitude higher than the permeability to water of concrete and cement mortars (Hall and Hoff 2002; Halamickova and Detwiler 1995; Ganjian et al. 2006; Scherer et al. 2007; Wongpa et al. 2010). When the measurement was repeated many times on the same sample, the K_h value decreased, because of the action of water that, passing through a partially carbonated mortar, dissolved the portlandite still present in the sample and possibly leached this phase, leading to its re-precipitation in other zones of the pore network. This means that the pore system is modified by the continuous flux of water and therefore the hydraulic conductivity of the material too. However, it was not possible to confirm this hypothesis, since a mineralogical or textural analysis of the whole sample can hardly give a real mapping of the portlandite in it. In addition to this, it is worth remembering that this phase turns into calcium carbonate when the sample is in contact with air, namely during the necessary drying of the sample before XRD, MIP and SEM analyses. Even so, the dependence of the hydraulic conductivity on time was already observed by Hall and Hoff (2002).

According to the final values of hydraulic conductivity found for the four mortar types (K_h, in Table 3), this parameter decreases exponentially with the B/A ratio of the mortar (Fig. 6a), which means that there is an exponential increase for increasing volume of the aggregate. This is in agreement with the general observation that concrete presents higher hydraulic conductivity values than the corresponding cement paste (i.e. without aggregate) (Halamickova and Detwiler 1995), and it also confirms the importance of the interfacial transition zone (ITZ, zone between the grain surface and the matrix) on the permeability of a mortar to water (Scherer et al. 2007). However, the relationship obtained between hydraulic conductivity and porosity of mortars is not very clear. As shown in Fig. 6b, the permeability value increases for decreasing porosity from CCMPCR3 to CCMPCR6 mortars. Notwithstanding, this trend is not followed by CCMPCR9 mortar that presents a three times higher permeability value, even if its porosity is very similar to that of CCMPCR6 mortar. Moreover, CCMPCR9 is the only mortar that presented such a high dispersion of values (Fig. 6; Table 3). To interpret this controversial trend between the pore volume and the permeability value in CCMPCR9 mortar, we must consider that in mortars with high content of aggregate, the cohesion between grains and matrix is often scarce and this can lead to desegregation of the material with poor mechanical properties (Arizzi and Cultrone 2012). This low cohesion results in a wider interfacial transition zone, then in a higher porosity in this zone. However, the porosity at the ITZ is not easily detected by MIP analysis because the high pressure of mercury during the measurement can cause the detachment of the grains from the mortar sample, thus eliminating this interfacial porosity. This explains the low volume of pores with radius greater than 1 μm found in CCMPCR9 mortar (Arizzi and Cultrone 2012). If we consider the microstructural characteristics of CCMPCR9 mortars, we understand that the water flow is more favoured in this mortar because the water moves preferentially through the pores present in the ITZ zone. This also suggests that the tortuosity of these pores is lower than that of the capillary pores of the matrix (those with radius comprised between 0.1 and 1 μm), through which the water is preferentially absorbed by capillarity.

These findings confirm that the permeability of a material to water cannot be correctly determined on the basis of its open porosity (Anderson 1926) especially if we consider that K_h is measured on saturated samples, whilst porosity is determined after drying (Scherer et al. 2007). The most correct parameters that must be considered in the interpretation of the permeability to water are the pore size and tortuosity of the material, although these are sometimes underestimated by means of the MIP technique.

Table 3 Results of the permeability tests on mortars: values of hydraulic conductivity (water permeability, K_h, in ms^{-1}) and water vapour permeability (K_v, $gm^{-2}h^{-1}$)

Mortar name	$K_{h\ exp}$	K_v
CCMPCR3	1.2×10^{-6} (0.07×10^{-6})	2.65 (0.10)
CCMPCR4	5.1×10^{-6} (0.69×10^{-6})	2.87 (0.09)
CCMPCR6	7.5×10^{-6} (0.68×10^{-6})	2.69 (0.08)
CCMPCR9	21.8×10^{-6} (4.9×10^{-6})	3.09 (0.18)

Standard deviation is shown in *round brackets*

Water vapour permeability

Figure 7 shows the lineal weight drop of the samples subject to the water vapour permeability test. All mortars showed a very similar behaviour to water vapour, with some exception for CCMPCR9, whose curve has a sharper slope with respect to the others.

The water vapour permeability values measured in the four mortar types (Table 3) did not show a tight

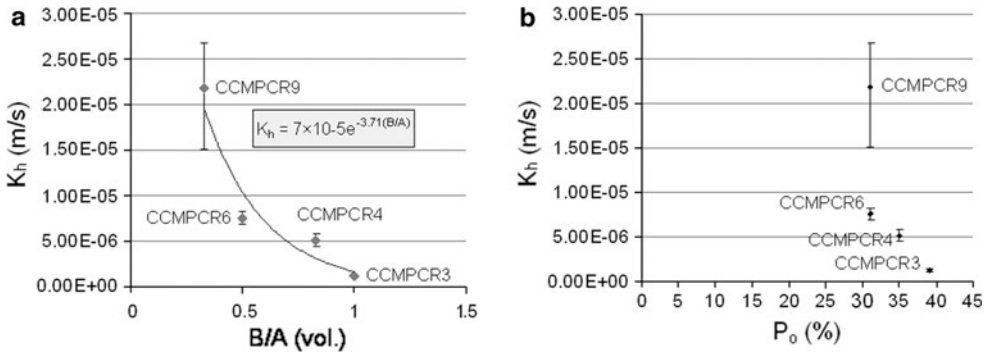

Fig. 6 Hydraulic conductivity values (K_h, m/s) are plotted against the binder-to aggregate ratio (B/A, by volume) (**a**) and the open porosity (P_o, in %) (**b**) of each mortar. In **a** the *continuous line* represents the exponential function found between hydraulic conductivity (K_h, in m/s) and B/A. *Error bars* represent the standard deviation determined on three samples per each mortar

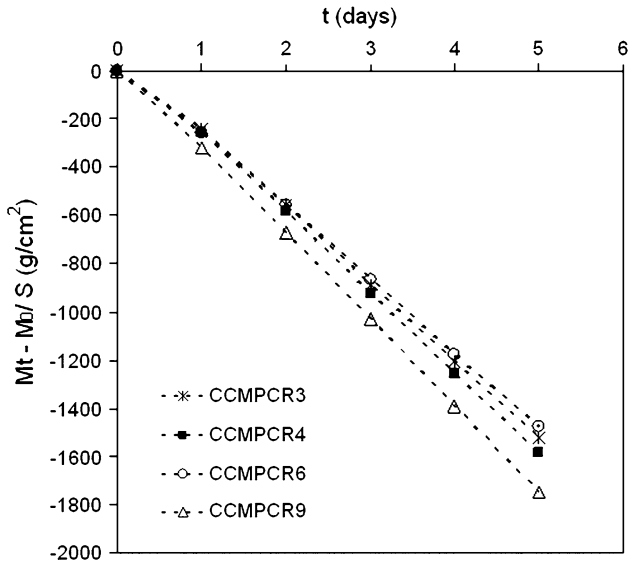

Fig. 7 Weight variation per surface unit ($M_t - M_0/S$, g/cm^2) of the four mortar types as function of time (t, days) during the water vapour permeability test

relationship neither with the aggregate content nor with the open porosity of each mortar (Table 2). In fact, although K_v seems to increase for increasing aggregate volume, as for the hydraulic conductivity (K_h), there is some discrepancy in the case of CCMPCR6, whose K_h value is too low when compared with the apparent trend followed by the other mortars. In fact, a very close behaviour to water vapour is observed in the curves of CCMPCR3, CCMPCR4 and CCMPCR6 mortars (Fig. 7).

It is known that the vapour diffusion through a material (i.e. stone, brick, mortar) depends on its microstructural characteristics, especially the pore network (main pore size and shape) (Quenard and Sallee 1992; Dondi et al. 2003; Johannesson 2002). Since the pore size of the four mortars is almost the same [the main pore radius comprised between 0.1 and 1 μm (Arizzi and Cultrone 2012)], we can assume that the most relevant factor on the water vapour permeability of aerial lime-based mortars is the pore tortuosity, which is reduced by the presence of the aggregate, as discussed in "Hydraulic conductivity".

In the same way as found for water vapour, it can be expected that the CO_2 diffusion within mortars with high content of aggregate is faster (and the carbonation enhanced). Notwithstanding, we observed in a previous study (Arizzi et al. 2012) that mortars with high aggregate proportion were the least carbonated after several days of exposure to weathering conditions. This occurred because carbonation process leads to continuous changes in the microstructure of mortars, which lie in the closure of the pores due to the precipitation of calcite, that reduce the mortar permeability to CO_2. Mortars with high aggregate content suffer a higher decrease of the CO_2 diffusion during time because calcite precipitates preferentially at the interface between aggregate grains and matrix (at the interfacial transition zone) (Lawrence et al. 2007), where CO_2 diffusion is higher (Bourdette et al. 1995).

Shrinkage of mortars

Figure 8 shows the shrinkage curves of the four mortars studied, determined within a week, whilst the inset in Fig. 8 shows the shrinkage occurred during the first 24 h. The shrinkage is almost the same (0.5 mm) in all mortars within the first 4 h. After this period, CCMPCR3 mortar presents a higher volume reduction (4 mm) compared to the other mortars (1.3–1.9 mm), as reflected in the shrinkage coefficients (Table 4). This high volume reduction, which was expected in CCMPCR3 being the mortar with the highest lime content, achieved a quite constant value after 12 h. However, CCMPCR3 showed a different shrinkage curve with respect to CCMPCR4, CCMPCR6 and CCMPCR9 mortars (Fig. 8). The sharp slope of its curve can be related indirectly to the effectiveness of the cellulose derivative as water-retaining agent. As shown in Table 1, the same amount of admixtures was added in each mortar, independently on the binder amount. However, it is possible that the amount of cellulose derivative added in CCMPCR3 mortar is not enough to improve the water-retention capacity of the lime, which is in higher content in this mortar, then to counteract its shrinkage. In the other mortars, instead, the water-reducing agent seems to be able

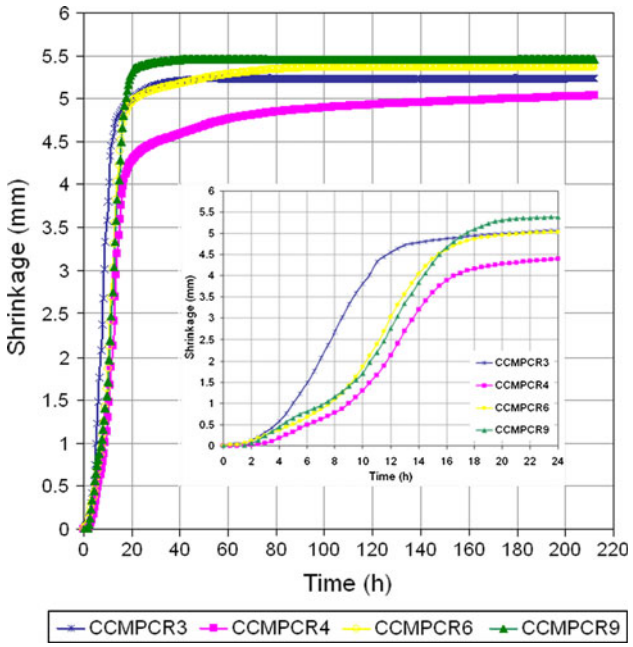

Fig. 8 Shrinkage curves of mortar samples during 7 days. The *inset* shows the shrinkage curves within the first 24 h

Table 4 Shrinkage measurements in mortars: shrinkage coefficient (C_{shr}, mm/h) determined after 12 h and values of the final shrinkage (in %) measured on the length of the samples

Mortar name	C_{shr}	Final shrinkage (%)
CCMPCR3	0.34	1.31
CCMPCR4	0.12	1.26
CCMPCR6	0.18	1.34
CCMPCR9	0.17	1.36

to reduce the water evaporation rate but within a limited period of time (approximately 10 h). In fact, CCMPCR9 reached the highest shrinkage after 1 day, CCMPCR6 showed a continuous increase until the fifth day, reaching a value of shrinkage similar to CCMPCR9 and higher than CCMPCR3, and the volume reduction in CCMPCR4 still increased during the following days, but it achieved a lower value than in the other mortars (Table 3).

Considering these results, we interpret that different factors contribute to the development of shrinkage fissures in these types of mortars. The most important one is related to the amount of kneading water needed for the elaboration of mortars and it shows its effect during the first few hours of drying. Mortars with higher water content undergo a much higher shrinkage in the first few hours, such as the case of CCMPCR3 mortar. A secondary factor is probably related with the degree of cohesion exhibited between aggregate and matrix during the first few days of hardening. The low cohesion that characterises CCMPCR9 mortar would explain the slightly highest shrinkage achieved in this mortar at the end of the test.

However, the differences between the shrinkage values of these mortars are very little, considering that the final dimensional variations of the samples are almost equal (between 1.3 and 1.4 % of the total length of the sample).

Conclusions

Studying the water transfer properties and drying shrinkage of lime-based mortars with different binder-to-aggregate ratios has helped understand which many microstructural aspects of a mortar affect its hygric behaviour. In particular, we have demonstrated that, although the hygric parameters obtained for mortars of same composition are very similar, some differences exist according to their microstructure, which is slightly modified by the aggregate content.

Firstly, it has been found that the mortar with the highest lime content (CCMPCR3) was more susceptible to the water uptake by free immersion and capillarity; it generally showed higher water content at the end of these tests. The mortar with the highest aggregate content (CCMPCR9) presented, instead, a faster drying and a higher permeability to water and water vapour. Both findings are related with the microstructure and pore network of these mortars. In mortars with higher content of lime, the open porosity of the matrix is high and this explains the higher water content absorbed by the capillary pores. In mortars with higher content of aggregate, the low cohesion between matrix and aggregate grains generates some porosity at the interfacial transition zone that gives place to much higher permeability to water and water vapour compared to mortars with higher lime content.

Secondly, the shrinkage of mortars turned out to be quite different from the expected, being the highest in the CCMPCR9 and not in CCMPCR3, which was prepared with the highest amount of lime and water. This has been related again to the scarce cohesion of this mortar.

Finally, it has been taken into account that the microstructure of "young" (i.e. partially carbonated) mortars is subjected to slight modifications led by the carbonation process, which is still on-going, as well as by the dissolution of portlandite in water and the occurrence of hydration reactions between the reactive phases of metakaolin and water. These processes could make the results of this work meaningless, unless they are merely assumed for comparative purposes when it is necessary to select the right mix among several ones. Moreover, in a building, the mortar is exposed to water and water vapour since its very early age, that is, when it is more vulnerable to weathering conditions. For this reason, it is important to

choose the mortar mix that shows the best water transfer properties when it is not yet fully carbonated. The improvement of the physical properties of a mortar led by the carbonation process guarantees that the mortar selected will show better hygric behaviour over time.

As general conclusion, the CCMPCR6 showed one of the lowest values of free water absorption and capillary uptake; the CCMPCR4 mix, instead, showed one of the best drying behaviours and the lowest values of shrinkage, as well as one of the highest values of permeability to water vapour. From this, we envisage that a binder-to-aggregate proportion between 1:4 and 1:6 would be the most suitable for a repair rendering mortar, considering the compatibility requirements discussed above for this type of building material. This conclusion reinforces our previous statements (Arizzi and Cultrone 2012; Arizzi et al. 2012) regarding the appropriate binder-to-aggregate dosage to be used in mortars designed for rendering purposes.

It is evident from this research and our previous works that there exist general mixing rules that should be followed for the correct design of a mortar. In first place, it is important to bear in mind the characteristics required according to the intended function of the mortar in the masonry. In second place, once chosen the most suitable components for the specific mortar, it is preferable to prepare different mixes and perform a mineralogical, textural and physical–mechanical characterisation of them, so as to be able to select the most suitable aggregate dosage for each mortar composition. Although carrying out a detailed study of compatibility and suitability of the repair materials entails higher initial costs and longer times, this is the only way of ensuring an appropriate and durable repair intervention.

Acknowledgments This study was financially supported by Research Group RNM179 of the Junta de Andalucía and by Research Project P09-RNM-4905. We are grateful to Dr. Mona Edwards (University of Oxford, UK) for her assistance in the use of the falling head permeameter and to ARGOS Derivados del Cemento S.L (Granada, Spain) for supplying the raw materials and for the use of SWG-H-400 shrinkage-measuring device.

References

Anderson E (1926) Relation between water permeability and water absorption of concrete. Industrial and Engineering Chemistry

Arizzi A, Cultrone G (2012) Aerial lime-based mortars blended with a pozzolanic additive and different admixtures: a mineralogical, textural and physical–mechanical study. Constr Build Mater 31:135–143

Arizzi A, Martínez-Martínez J, Cultrone G, Benavente D (2011) Mechanical evolution of lime mortars during the carbonation process. Key Eng Mater 465:483–486

Arizzi A, Viles H, Cultrone G (2012) Experimental testing of the durability of lime-based mortars used for rendering historic buildings. Constr Build Mater 28:807–818

Arizzi A, Martínez-Martínez J, Cultrone G (2013) Ultrasonic wave propagation through lime mortars: an alternative and non-destructive tool for textural characterization. Mater Struct. doi: 10.1617/s11527-012-9976-1 (in press)

ASTM C618-08 (2008) Standard specification for coal fly ash and raw or calcined natural pozzolan for use in concrete. In: Annual Book of ASTM Standard. ASTM International Standards Worldwide, Pennsylvania

Beck K, Al-Mukhatar M, Rozenbaum O, Rautureau M (2003) Characterization, water transfer properties and deterioration in tuffeau: building material in the Loire valley-France. Build Environ 38:1151–1162

Benavente D, Lock P, García del Cura MA, Ordóñez S (2002) Predicting the capillary imbibition of porous rocks from microstructure. Transp Porous Med 49:59–76

Benavente D, Cañaveras JC, Cuezva S, Laiz L, Sanchez-Moral S (2009) Experimental definition of microclimatic conditions based on water transfer and porous media properties for the conservation of prehistoric constructions: Cueva Pintada at Galdar, Gran Canaria, Spain. Environ Geol 56:1495–1504

Bourdette B, Ringot E, Ollivier JP (1995) Modelling of the transition zone porosity. Cem Concr Res 25(4):741–751

Cazalla O (2002) Morteros de cal. Aplicación en el Patrimonio Histórico, PhD thesis, Universidad de Granada, Spain

Cultrone G, Sebastián E (2008) Laboratory simulating showing the influence of salt efflorescence on the weathering of composite building materials. Environ Geol 56:729–740

De La Torre MJ (2003) Caracterización de las propiedades hídricas de los materiales lapídeos. In: Villegas R, Eduardo M, Sebastian P (eds) Cuadernos Técnicos, Metodología de diagnóstico y evaluación de tratamientos para la conservación de los edificios históricos, pp 104–111

Domenico PA, Schwartz FW (1990) Physical and chemical hydrogeology. Wiley, New York

Dondi M, Principi P, Raimondo M, Zanarini G (2003) Water vapour permeability of clay bricks. Constr Build Mater 17:253–258

Frías M, Sánchez de Rojas MI, Cabrera J (2000) The effect that the pozzolanic reaction of metakaolin has on the heat evolution in metakaolin-cement mortars. Cem Concr Res 30:209–216

Ganjian E, Claisse P, Tyrer M, Atkinson A (2006) Factors affecting measurement of hydraulic conductivity in low-strength cementitious materials. Cem Concr Res 36:2109–2114

Groot CJWP (2010) Performance and repair requirements for renders and plasters. In: International workshop on "Repair mortars for historic masonry", RILEM TC 203-RHM, Prague

Groot C, Gunneweg JTM (2010) The influence of materials characteristics and workmanship on rain penetration in historic fired clay brick masonry. Heron 55(2):141–154

Halamickova P, Detwiler RJ (1995) Water permeability and chloride ion diffusion in Portland cement mortars: relationship to sand content and critical pore diameter. Cem Concr Res 25(4):790–802

Hall C, Hoff WD (2002) Water transport in brick, stone and concrete. Taylor and Francis, London

Hall C, Hoff WD (2007) Rising damp: capillary rise dynamics in walls. Proc R Soc 463:1871–1884

Hughes JJ (2010) The role of mortar in masonry: an introduction to requirements for the design of repair mortars. In: International workshop on "Repair mortars for historic masonry", RILEM TC 203-RHM, Prague

Ingham JP (2005) Predicting the frost resistance of building stone. Q J Eng Geol Hydrogeol 38:387–399

Johannesson BF (2002) Prestudy on diffusion and transient condensation of water vapour in cement mortar. Cem Concr Res 32:955–962

Lanas J, Alvarez JI (2003) Masonry repair lime-based mortars: factors affecting the mechanical behavior. Cem Concr Res 33:1867–1876

Lawrence RM, Mays TJ, Rigby S, Walker P, D'Ayala D (2007) Effects of carbonation on the pore structure of non-hydraulic lime mortars. Cem Concr Res 37:1059–1069

Mamillan M (1981) Connaissances actuelles des problemes de remontées d'eau par capillarite dans les murs. In: Preprints of the contributions to the international symposium: The conservation of stone II. Centro per la Conservazione delle Sculture all'aperto. Bologna, pp 59–72

Maurenbrecher AHP (2004) Mortars for repair of traditional masonry. Practice periodical on structural design and construction 9(2):62–65

NORMAL 21/85 (1985) Permeability to water vapour. CNR-ICR, Rome

NORMAL 29–88 (1988) Drying index measure. CNR-ICR, Rome

Quenard D, Sallee H (1992) Water vapour adsorption and transfer in cement-based materials: a network simulation. Mater Struct 25:515–522

Rojo A, Alonso FJ, Esbert RM (2003) Hydric properties of some Iberian ornamental granites with different superficial finishes: a petrophysical interpretation. Mater Constr 53(269):61–72

Rose DA (1963a) Water movement in porous materials: Part 1-Isothermal vapour transfer. Brit J Appl Phys 14:256–262

Rose DA (1963b) Water movement in porous materials: Part 2-The separation of the components of water movement. Brit J Appl Phys 14:491–496

Ruiz-Agudo E, Lubelli B, Sawdy A, van Hees R, Price C, Rodriguez-Navarro C (2011) An integrated methodology for salt damage assessment and remediation: the case of San Jerónimo Monastery (Granada, Spain). Environ Earth Sci 63(7):1475–1486

Scherer GW (1990) Theory of drying. J Am Cer Soc 73:3–14

Scherer GW, Valenza JJ II, Simmons G (2007) New methods to measure liquid permeability in porous materials. Cem Concr Res 37:386–397

Szemerey-Kiss B, Torok A (2011) Time-dependent changes in the strength of repair mortar used in the loss compensation of stone. Environ Earth Sci 63(7–8):1613–1621

UNE EN 1015-11 (1999) Methods of test for mortar for masonry. Part 11: determination of flexural and compressive strength of hardened mortar. AENOR, Madrid

UNE EN 1015-3 (1999) Methods of test for mortar for masonry. Determination of consistence of fresh mortar by flow table, AENOR

UNE EN 459-1 (2002) Description building lime. Part 1: definitions, specifications and conformity criteria. AENOR, Madrid

UNI EN 1925 (2000) Natural stone test methodsdetermination of water absorption by capillarity. CNR-ICR, Rome

UNI-EN 13755 (2008) Natural stone test methodsdetermination of water absorption at atmospheric pressure. CNR-ICR, Rome

Veiga MR (2010) Conservation of historic renders and plasters: from lab to site. In: Proceedings of the 2nd historic mortars conference, Prague

Vos BH (1978) Hydric methods for the determination of the behaviour of stones. In: Proceedings of the UNESCO-RILEM international symposium, Paris

Warscheid Th, Braams J (2000) Biodeterioration of stone: a review. Int Biodeter Biodegr 46:343–368

Wongpa J, Kiattikomol K, Jaturapitakkul C, Chindaprasirt P (2010) Compressive strength, modulus of elasticity, and water permeability of inorganic polymer concrete. Mater Des 31:4748–4754

Wood C (2010) Understanding and controlling the movement of moisture through solid stone masonry caused by driving rain. MSc Thesis, University of Oxford, UK